- 1 The Role of Solar Photolysis in the Atmospheric Removal of Methacrolein
- 2 Oxide and the Methacrolein Oxide-Water van-der Waals Complex in Pristine
- 3 Environments
- 4 Lily M. Guidry, Londyn A. Bardash, Aylin Yigiter, 2 Satyam Ravi, Barbara Marchetti, 4 and
- 5 Tolga N. V. Karsili^{1,*}
- ¹University of Louisiana at Lafayette, Lafayette, 70503, USA
- ²St. Thomas More Catholic High School, Lafayette, 70508, USA
- ³School of Advanced Science and Languages, VIT Bhopal University, Kothrikalan, Sehore,
- 9 Madhya, Pradesh, 466114 India
- *Author to whom correspondence should be addressed: Barbara.marchetti@louisiana.edu;
- 11 tolga.karsili@louisiana.edu

12 Abstract

- Biogenic hydrocarbons are emitted into the Earth's atmosphere by terrestrial vegetation as
- biproducts of photosynthesis. Isoprene is one such hydrocarbon and is the second most abundant
- volatile organic compound emitted into the atmosphere (after methane). Reaction with ozone
- represents an important atmospheric sink for isoprene removal, forming carbonyl oxides
- 17 (Criegee intermediates) with extended conjugation. In this manuscript we argue that the extended
- conjugation of these Criegee intermediates enables electronic excitation of these compounds, on
- 19 timescales that are competitive with their slow unimolecular decay and bimolecular chemistry.
- We show that the complexation of MACR-oxide with water enhances the absorption cross
- section of the otherwise dark S₁ state, potentially revealing a new avenue for forming lower
- volatility compounds via tropospherically relevant photochemistry.

Introduction

Isoprene is the most abundant biogenic volatile organic compound (BVOC) emitted into the troposphere (500 Tg per year) by terrestrial vegetation.¹ During daytime, the atmospheric lifetime of isoprene is ca. 1-2 hours, which is limited by reaction with oxidants such as the OH radical (ca. 80 %) and O₃ (ca. 10 %).²

Figure 1: Ozonolysis reaction of isoprene and the resulting products.

Following bimolecular interaction, O₃ undergoes a thermally allowed [3+2]-cycloaddition reaction across one of the two double bonds of isoprene, as illustrated in Fig. 1. Three different CIs, formaldehyde oxide (CH₂OO), methyl vinyl ketone oxide (MVK-oxide), and methacrolein oxide (MACR-oxide), are formed.²⁻⁵ MACR-oxide will be the focus of this article. Once formed, the nascent MACR-oxide is highly internally excited and may undergo unimolecular decay or collisions with proximal bath gases to become collisionally stabilized. In terminal CIs, such as

37 CH₂OO and MACR-oxide, unimolecular decay is governed by cyclization to form cyclic dioxo-

compounds.4,6 38

39

40

41

42

43

44

45

46

47

48

49

50

51

52

53

54

55

As with other alkyl substituted CIs, the unimolecular decay of the lowest energy syn-trans conformer of MVK-oxide is dominated by intramolecular 1,4-H-atom transfer (1,4-HAT) to form a stable but internally excited vinyl hydroperoxide (VHP) that rapidly decomposes to form OH + vinoxy radical products. Recent studies have also identified a unimolecular cyclization to forming dioxole products, which is only possible in the *anti-trans* conformer.^{7,8} This indicates that the higher energy conformers may also be formed in experiments and during ozonolysis. This may be understood by recognizing that the high internal energy of nascent CIs may lead to a non-Boltzmann distribution of conformers. Unlike CH2OO, in pristine humid conditions, bimolecular chemistry of MVK-oxide with water is slow, in line with other alkyl substituted CIs.9 In contrast, the lowest energy conformer of MACR-oxide is anti-trans. Unimolecular decay of MACR-oxide is comparatively slower as the equivalent 1,4-HAT path to forming a stable VHP is unavailable. Surprisingly MACR-oxide is stable in humid conditions, implying that its bimolecular chemistry with water is slow. 10 Both MVK-oxide and MACR-oxide contain extended conjugation when compared to smaller CIs such as CH₂OO.¹¹ As the UV-visible

electronic absorption and around a 4-fold increase in the absorption cross section (cf.

spectra in Fig. 2 show, this extended conjugation manifests in a bathochromic shift in their

CH₂OO). 12-15 56

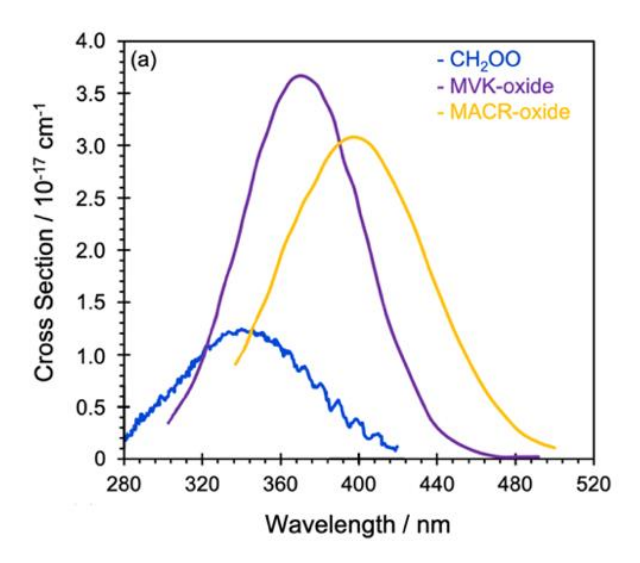


Figure 2: Experimentally measured electronic absorption spectrum reproduced, with permission, from refs. 14 and 15.

As with CH₂OO, the near-UV-visible absorption spectra of MVK-oxide and MACR-oxide are dominated by strongly absorbing $\pi\pi^*$ electronic states. ^{12,13,15–17} Recent Velocity Map Imaging (VMI) studies have revealed that excitation to the $\pi\pi^*$ state leads to oxygen atom products. ^{12,13,18} This can be understood by inspecting Fig. 3, which shows potential energy (PE) profiles of the lowest nine singlet electronic states of the lowest energy *anti-cis* conformer of MACR-oxide along the O-O stretch coordinate (R_{OO}). ¹⁸ The analogous PE profiles for MVK-oxide are very similar, with only subtle changes in the vertical excitation and asymptotic energies. The bright $\pi\pi^*$ (S₂) state is dissociative with respect to R_{OO} and adiabatically correlates with the O(1 D) + MVK/MACR (S₀) products at asymptotic O-O bond distances. A second asymptote, corresponding to the O(3 P) + MVK/MACR (T₁) products, is accessible at excitation energies greater than ca. 3.25 eV. Our recent collaborative work with the Lester group has revealed that excitation of CH₂OO at energies above the second asymptote limit leads to both O(3 P) and O(1 D) products. ¹⁹ Such results are profound since nascent O(1 D) products may react with water vapor to generate OH radicals in the

atmosphere. Additionally, the T₁ MVK/MACR products may react with atmospheric O₂ to form lower volatility compounds that may have implications on secondary organic aerosol formation.

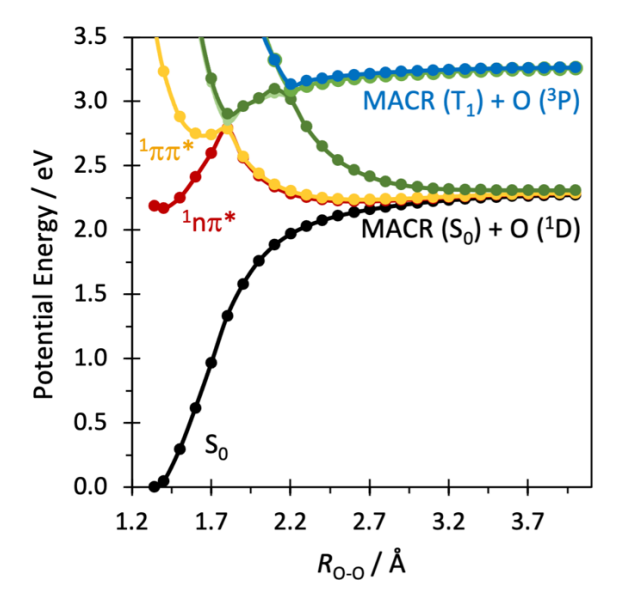


Figure 3: Adiabatic potential energy profiles of the lowest seven singlet electronic states along the O-O stretch coordinate of the lowest energy conformer of MACR-oxide.

In this manuscript, we will explore the extent to which solar photolysis contributes to the

In this manuscript, we will explore the extent to which solar photolysis contributes to the atmospheric removal of MACR-oxide and the MACR-oxide-water complex. We show that upon complexation with water, the resulting MACR-oxide-water complex primarily undergoes O-O bond fission. Interestingly, we show that the complexation of MACR-oxide with water enhances the absorption cross section of the otherwise dark S_1 state, potentially leading to a new avenue for forming lower volatility compounds via tropospherically relevant photochemistry.

Computational Methods

Using Gaussian 16,^{20,21} the ground state minimum energy geometry of MACR-oxide and its van der Waals complex with water monomer (MACR-oxide-H₂O) and water dimer (MACR-oxide-

(H₂O)₂) was optimized at the m062x/aug-cc-pVTZ level of theory.²² This level of theory has been previously shown to perform well for determining minimum energy geometries for Criegee intermediates.^{23,24} Similarly, the ground state minimum energy geometries of CH₂OO and MACR-oxide, along with their respective pre-reactive complexes with water monomer, hydroxyhydroperoxide products, and transition states along the CH₂OO/MACR-oxide + water monomer reaction coordinate were calculated at the same level of theory. Single point energies of the aforementioned optimized molecules were calculated at the CCSD(T)-F12/cc-pVTZ-F12 level of theory through Molpro 2022. The ground state minimum energy geometries and single point energies of the various unimolecular decay products of MACR-oxide (aldehyde, dioxirane, and acid products), both with and without complexation to water monomer, were calculated using the same aforementioned CCSD(T)-F12/cc-pVTZ-F12//m062x/aug-cc-pVTZ combination of theory. Using Molpro 2022,²⁵ vertical excitation energies (VEEs) and oscillator strengths were calculated using complete active space second-order theory (CASPT2)^{26–28} coupled to Dunning's augmented correlation-consistent basis set of triple-ζ quality: aug-cc-pVTZ.²⁹ These CASPT2 computations were based on a state-averaged complete active space self-consistent field (CASSCF)^{30,31} reference wavefunction. An active space of ten electrons in eight orbitals (displayed in the supporting information) was used. Trajectory surface hopping (TSH) simulations³² were performed using the Newton-X computational package.³³ Initial positions and momenta were sampled using a Wigner distribution, which was based on the aforementioned ground state minimum energy geometry calculated at the m062x/aug-cc-pVTZ level of theory. Due to the reliability of this level of theory, we believe that it proves as an adequate method to sample an accurate representation of the local of the ground state v=0 level. In the TSH simulations, the nuclear coordinates were

89

90

91

92

93

94

95

96

97

98

99

100

101

102

103

104

105

106

107

108

109

110

propagated by integrating Newton's equation using the velocity Verlet method, while the electronic coordinates were propagated by numerically solving the time-dependent Schrödinger equation using Butcher's fifth-order Runge-Kutta method in steps of 0.025 fs. A total of 100 trajectories were initiated in the S₂ state; the energies, gradients and non-adiabatic coupling matrix elements of the seven lowest singlet states were calculated analytically and "on-the-fly" using the SS-SR-CASPT2 method in coupled with the aug-cc-pVDZ basis set. SS-SR-CASPT2 enables the computation of energies and analytical gradients at MS-CASPT2 quality, at a reduced computational cost; it also performs well near electronic state degeneracies. ^{34,35} The SS-SR-CASPT2 calculations were based on a state-averaged complete active space self-consistent field (CASSCF) method reference wavefunction and the same active space as above. These were performed via the BAGEL interface to Newton-X. The state hopping probabilities were evaluated by calculating the non-adiabatic coupling matrix elements from the SS-SR-CASPT2 computations.

Additional CASPT2/aug-cc-pVTZ calculations (using the same active space as above) were performed in order to compute the relaxed energy profiles along the O-O stretch and out-of-plane torsional coordinates. These latter calculations were performed using Molpro.

Results and Discussion

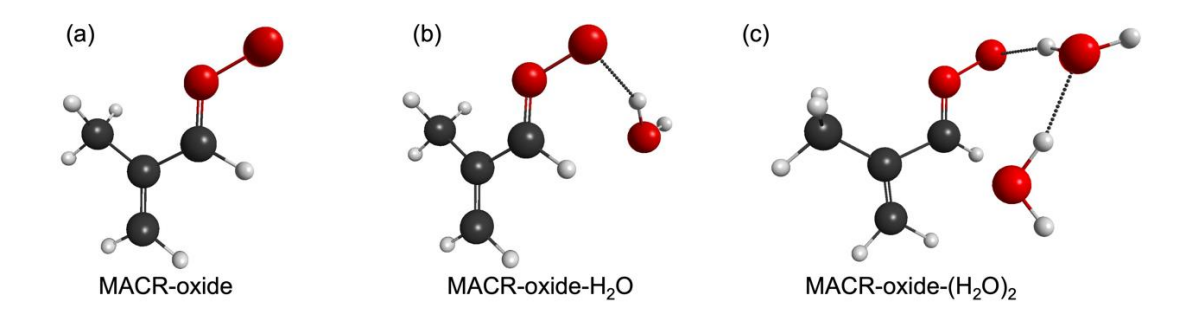


Figure 4: Lowest energy conformer of (a) MACR-oxide, (b) the MACR-oxide-H₂O complex, and (c) the MACR-oxide-(H₂O)₂ complex.

Fig. 4 displays the minimum energy geometries for the lowest energy conformers of isolated MACR-oxide, as well as the van der Waals (vdW) complexes formed with water monomer (Fig. 4(b)) and water dimer (Fig. 4(c)). These geometries have already been characterized in previous studies but are reintroduced here for orientation.

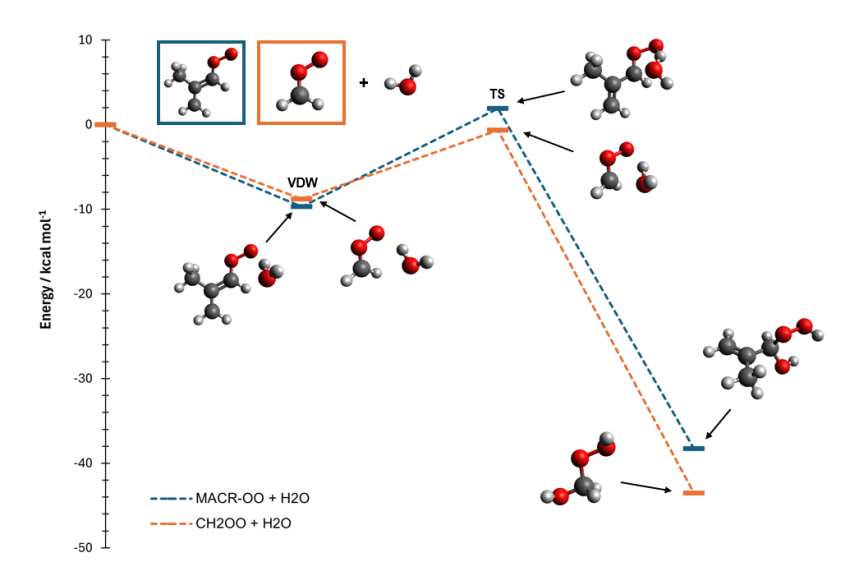


Figure 5: Energy profile associated with the reaction of CH₂OO and MACR-oxide with water monomer calculated at the CCSD(T)-F12/cc-pVTZ-F12//m062x/aug-cc-pVTZ level of theory.

As noted previously by us and others,¹³ the lowest energy structure of MACR-oxide is with the terminal oxygen atom orientated away from the carbon-framework and towards the aldehydic hydrogen atom. In this conformer, unimolecular decay is unsurprisingly slow as the only available path is a high barrier cyclization process that forms dioxirane.⁴ In CH₂OO, reaction with water dimer represents its dominant removal path.^{36–41} The analogous reaction of the lowest energy conformer of MACR-oxide with water is surprisingly slow.¹⁰ This can be understood by

inspecting Fig. 5, which shows that the calculated minimum energy profiles associated with MACR-oxide + water reaction includes a higher transition state barrier than the analogous profiles associated with the CH₂OO + water reaction. Given the slow unimolecular and bimolecular chemistry in pristine environments, we hypothesize that the nascent dispersively bound MACR-oxide-water monomer/dimer complexes (i.e., structures in Figs. 4(b) and 4(c)) survive for sufficiently long timescales that they undergo electronic excitation via absorption of tropospherically relevant solar radiation, on competitive timescales to thermal unimolecular decay and bimolecular chemistry.

Table 1: Vertical excitation energies (VEE) and oscillator strengths (in paratheses) of the various CIs studied in the present study, calculated at the CASPT2/aug-cc-pVTZ level of theory.

Criegee intermediate	VEE (oscillator strength) / eV		
	¹ nπ*-S ₀	¹ ππ*-S ₀	
CH ₂ OO	2.40 (0.0000)	3.91 (0.1022)	
CH ₂ OO-H ₂ O	2.84 (0.0004)	3.85 (0.0880)	
MACR-oxide	2.14 (0.0000)	3.29 (0.1080)	
MACR-oxide-H ₂ O	2.74 (0.0006)	3.27 (0.1509)	
MACR-oxide-(H ₂ O) ₂	2.94 (0.0006)	3.34 (0.1520)	

Table 1 lists vertical excitation energies and oscillator strengths associated with excitation to the lowest singlet states of CH₂OO and MACR-oxide, along with their vdW complexes with water monomer and water dimer. Alongside this table, Fig. 6 displays orbitals and orbital promotions that lead to the S₁ and S₂ electronic state configurations. In both CH₂OO and MACR-oxide, as well as their vdW complexes with water, the near-UV-visible absorption is dominated by

absorption to the S₂ state, which as Fig. 6 shows, involves a $\pi^* \leftarrow \pi$ orbital promotion. Since the participating orbitals have considerable spatial overlap, the associated oscillator strength is high. In contrast, the S_1 state involves a transition between non-bonding and π^* orbitals, manifesting in an S_1 state configuration of $n\pi^*$ character. The spatial overlap between the participating orbitals is minimal, manifesting in a dark state with low oscillator strength. Interestingly, although the oscillator strength accompanying the S₁ state transition of the CH₂OO-H₂O and the MACRoxide-H₂O vdW complex is also low, it is ca. 30 times stronger than isolated CH₂OO and MACR-oxide. This may be understood by recognizing the closer energetic proximity of the S₁ and S₂ state (v. Table 1) in the vdW complexes (cf. isolated CH₂OO and MACR-oxide). This would manifest in greater coupling between the S₁ and S₂ states, ultimately brightening the nominally dark S₁ state. This is supported by the configuration interaction (CI) coefficients in the returned CASPT2 calculations, which reveal that the S_1 state is primarily $\pi^* \leftarrow$ n character but with a strong contribution from the $\pi^* \leftarrow \pi$ excitation in the MACR-oxide-H₂O complex (0.04139). The analogous $\pi^* \leftarrow \pi$ CI coefficient for bare MACR-oxide is ca. two-orders of magnitude smaller (0.00015). The closer energetic proximity is plausibly explained by the large hypsochromic shift of the S₁ state absorption in the vdW complexes relative to isolated Criegee intermediates. This hypsochromic shift can be understood by recognizing that the terminal oxygen-centered n-orbital of the Criegee intermediate is stabilized upon hydrogen-bonding with water. Hydrogen-bonding is initiated by the interaction of this non-bonding lone-pair to the σ^* orbital localized around the O-H bond of water. The resulting n- σ^* interaction leads to stabilization of the n-orbital lone pair – thus increasing the n and π^* orbital energy gap relative to the isolated Criegee intermediate.

164

165

166

167

168

169

170

171

172

173

174

175

176

177

178

179

180

181

182

183

184

With this said, the effects of molecular symmetry pertaining to the CIs and CI-H₂O complexes discussed above are worthy of consideration. The stronger S₁ absorption cross-section of both the CH₂OO-H₂O and the MACR-oxide-H₂O vdW complex could plausibly be explained by the lowering of the molecular symmetry upon complexation (cf. bare CI). As S₁ excitation requires a change in the transition moment in the out-of-plane direction, the bare planar CIs of interest result in a dark S₁ state due to symmetry; this planar symmetry is thus broken when CH₂OO/MACR-oxide complex with H₂O. However, while molecular symmetry may contribute to the increased oscillator strength, both isolated CH₂OO and MACR-oxide computations were carried out without symmetry. Thus, there are no formal symmetry restrictions in the CASPT2 calculations performed. Once again drawing our attention to the orbital promotions highlighted in Fig. 6, it is apparent that there is poor spatial overlap of the orthogogonal orbitals associated with the S_1 state electronic transition ($\pi^* \leftarrow n$) in both isolated and complexed MACR-oxide. This leads to neglible and zero oscillator strength in the C₁ and C_s symmetry groups, respectively, in isolated CH2OO/MACR-oxide. As mentioned previously, the n-orbital localized on the terminal oxygen atom of MACR-oxide acts as the hydrogen bond donor participating in the $\pi^* \leftarrow$ n transition. The n-orbital donates electron density into the O-H centered σ^* orbital of water, which promotes hydrogen bonding and ultimately leads to polarization of the nominally in-plane n-orbital. This polarization can plausibly cause better spatial overalp between the n and π^* orbitals, possibly increasing $S_1 \leftarrow S_0$ absorption cross section. The consequence of a stronger S₁ state absorption in the MACR-oxide-H₂O complex is significant, since its vertical excitation energy overlaps significantly with the tropospherically relevant solar irradiance spectrum. As such, the long wavelength edge of the UV-visible spectrum of MACR-oxide in humid conditions may contain a weak underlying absorption to the

186

187

188

189

190

191

192

193

194

195

196

197

198

199

200

201

202

203

204

205

206

207

S₁ state, photoexcitation to which may be an important sink for vdW complexes. Although complexation and reaction of CIs with water dimer is more relevant than water monomer, given the similar vertical excitation energies and oscillator strengths of MACR-oxide-H₂O and MACR-oxide-(H₂O)₂, we will only consider the evolving dynamics of MACR-oxide-H₂O, in order to alleviate the higher computational cost of the MACR-oxide-(H₂O)₂ complex.

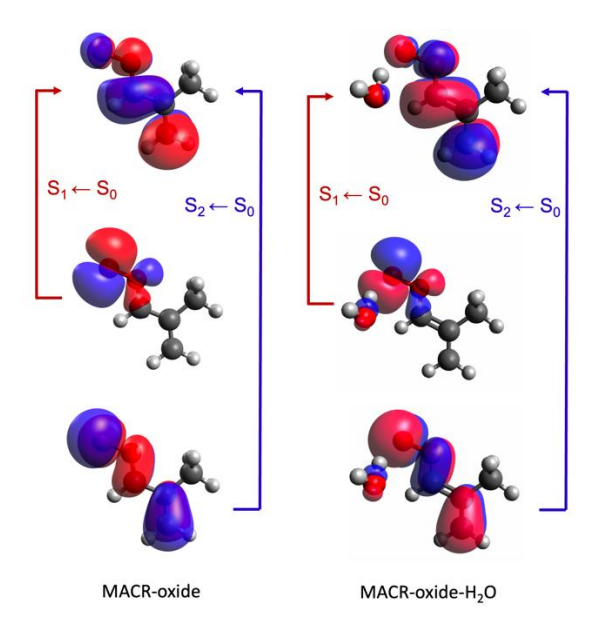


Figure 6: Orbitals and orbital promotions associated with excitation to the S₁ and S₂ states of MACR-oxide (left) and MACR-oxide-water (right).

We now turn our attention to comparing the excited state dynamics of MACR-oxide and the MACR-oxide-H₂O complex. Fig. 7 displays the normalized populations as a function of time obtained from the trajectory simulations of MACR-oxide (left) and MACR-oxide-H₂O (right) when initiated on the S₂ state. The internal energy distributions of the simulations is displayed in Figure S2. As evident from Fig. 7, the S₂ state in both MACR-oxide and MACR-oxide-H₂O depopulates within ca. 20 fs – which is driven primarily by internal conversion to the S₁ state. Within the next 20 – 40 fs, internal conversion is primarily to the S₁ state, with a minor component undergoing internal conversion to the S₀, S₃, S₄ states. Guided by the PE profiles in

Fig. 3, population transfer into the S_3 and S_4 states involves internal conversion from S_2/S_1 . This unusual energy transfer process involves population transfer to higher excited states than is usually observed in molecular photochemistry. In contrast, the early time population transfer to the S_0 state primarily involves evolution along the S_1 state, followed by internal conversion to the S_0 state at $R_{OO} > 2.0$ Å.

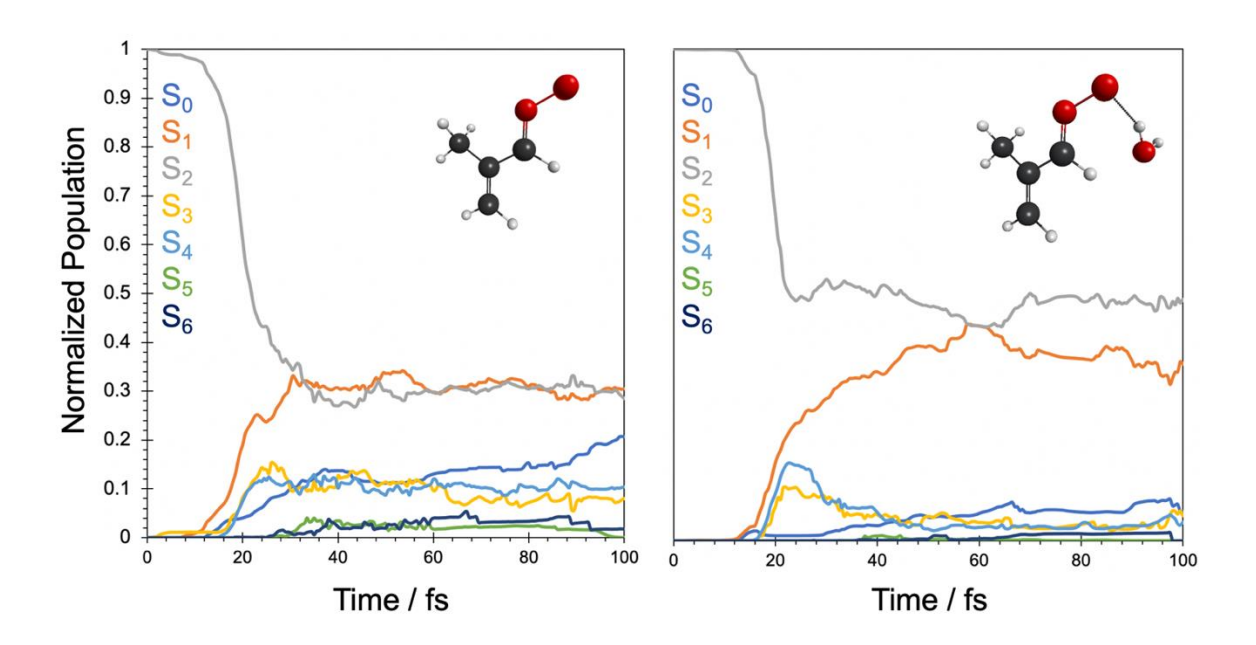


Figure 7: Time evolution of population between the lowest seven singlet states following excitation to the S₂ state of MACR-oxide (left) and MACR-oxide-H₂O (right).

The most obvious differences between the MACR-oxide and MACR-oxide-H₂O trajectories are observed at t > 30 fs, where the combined population in the S₀, S₃, and S₄ states is ca. 20 % lower in the MACR-oxide-H₂O complex than in bare MACR-oxide. Additionally, the combined population in the S₁ and S₂ states is ca. 80% (MACR-oxide-H₂O) and 60% (MACR-oxide) at 100 fs. Since the S₁ and S₂ states adiabatically correlate with the O(1 D) + MACR (S₀) products (see PE profiles in Fig. 3), trajectories that remain on these states may either remain as parent S₁ or S₂ molecules or undergo dissociation/isomerization on a longer timescale. As Fig. 8 shows,

the majority of trajectories undergo dissociation to form O + MACR products, while the rest remain as parent molecules. In comparing bare MACR-oxide with the MACR-oxide-H₂O complex, the latter shows a greater fraction (around 20%) of trajectories remaining as parent molecules at 100 fs. Guided by the population analysis in Fig. 7 and the branching fractions in Fig. 8, it is clear that the 20% higher population in the S₁ and S₂ states at 100 fs is primarily attributable to a greater fraction of the photoexcited MACR-oxide-H₂O complex remaining as parent molecules. This is reinforced by Table 2, which lists bond dissociation energies (D_0) for forming O(¹D) + CH₂O/MACR (S₀) and O(³P) + CH₂O/MACR (T₁) products for bare CH₂OO and MACR-oxide, as well as the MACR-oxide-H₂O complex. The latter D₀ value was obtained by taking the zero-point energy corrected energy difference between infinitely separated MACR + O + H₂O relative to the MACR-oxide-H₂O complex. As outlined above, the S₁ and S₂ states adiabatically correlate with the O (1 D) + CH₂O/MACR (S₀) products, but diabatically correlate with the O (3 P) + CH₂O/MACR (T_{1}) product limit. The D_{0} values for forming both products are higher for the MACR-oxide-H₂O complex than MACR-oxide, while the S₂ vertical excitation energy between the two systems remains largely unchanged. As such, the S₁ and S₂ minima are expected to be deeper in MACR-oxide-H₂O (cf. MACR-oxide) thus trapping more of the evolving population as parent S_1 and S_2 excited molecules.

242

243

244

245

246

247

248

249

250

251

252

253

254

255

256

257

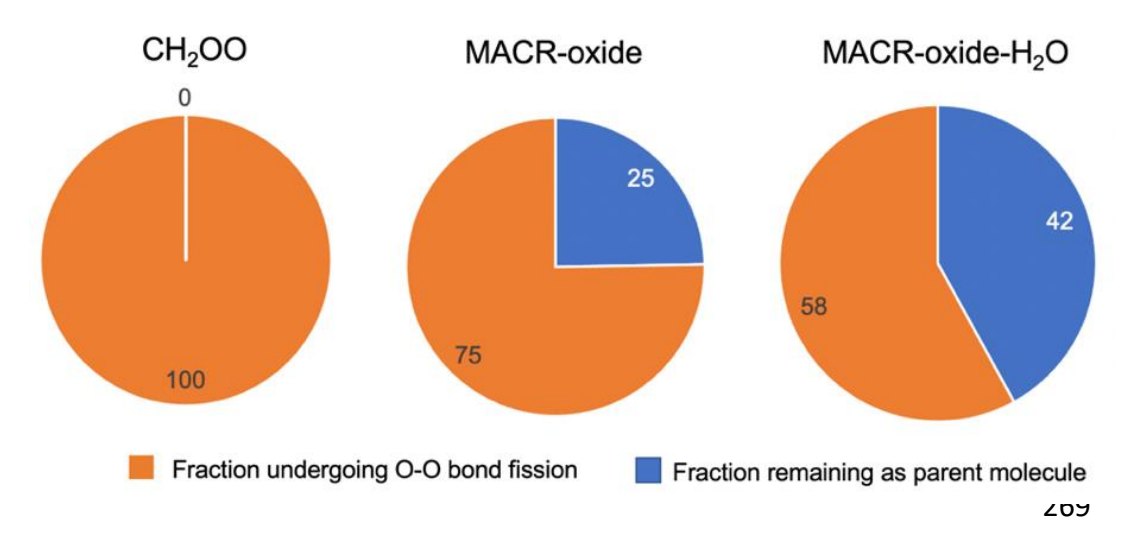


Figure 8: Fraction of population undergoing O-O bond fission *versus* remaining as parent molecules. Trajectories are analyzed at 100 fs.

Table 2: Minimum-to-minimum (D_e) and anharmonic zero-point corrected (D₀) bond dissociation energies of the two product channels are calculated at the CCSD(T)-F12b/cc-pVTZ-F12 level of theory. All energies are in eV.

Criegee intermediate	$O(^{1}D) + R'R''CO(S_{0})$		$O(^{3}P) + R'R''CO(T_{1})$	
	D _e	$\mathbf{D_0}$	$\mathbf{D}_{\mathbf{e}}$	$\mathbf{D_0}$
CH ₂ OO	2.51	2.39	3.58	3.37
MACR-oxide	2.55	2.45	3.59	3.39
MACR-oxide-H ₂ O	2.95	2.78	3.99	3.72

While MACR-oxide shows some population in the S_5 and S_6 states, these states are quenched in the MACR-oxide-H₂O complex. Since both states adiabatically correlate with the O (3 P) + CH₂O/MACR (T_1) asymptotic products, this quenching of population in S_5/S_6 can be understood by the higher D_0 for forming the O (3 P) + CH₂O/MACR (T_1) products in MACR-oxide-H₂O and thus a steeper gradient for accessing the S_5 and S_6 states from the vertically excited S_2 state.

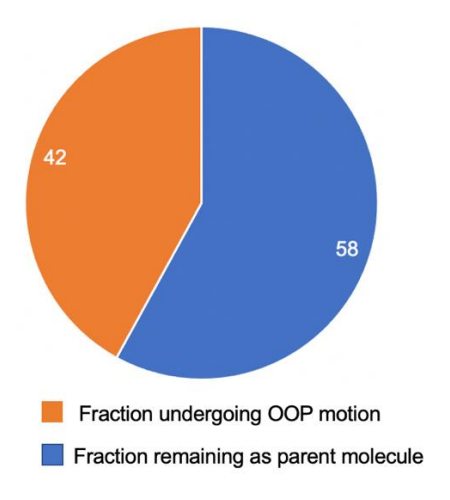


Figure 9: Fates of the evolving population following electronic excitation to the S₁ state of the MACR-oxide-H₂O complex.

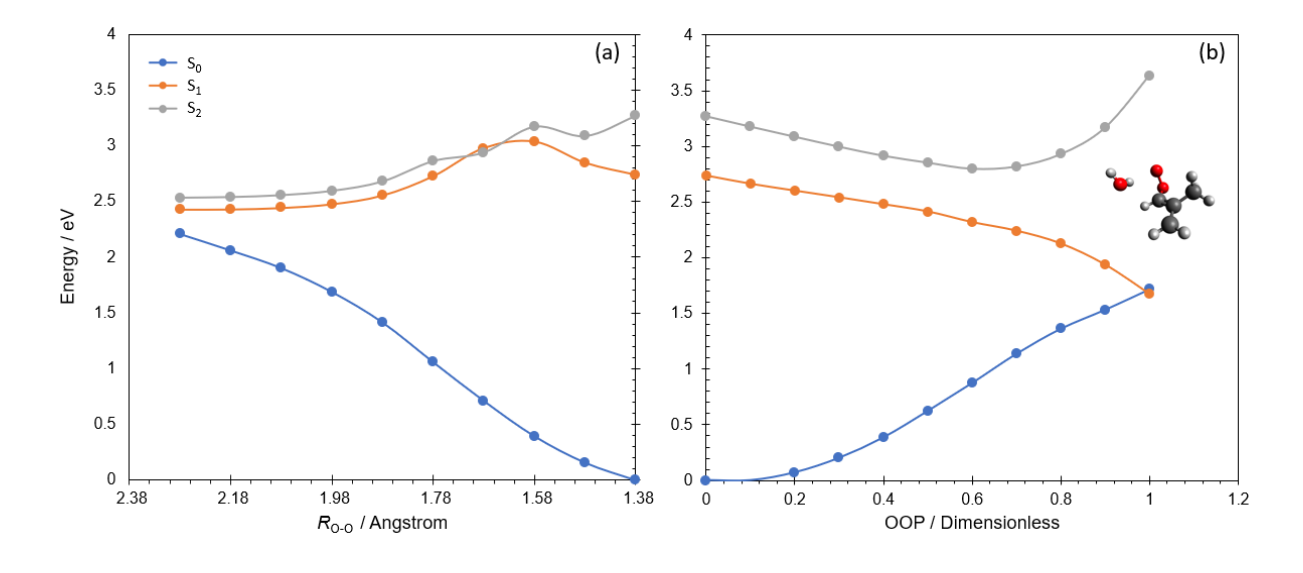


Figure 10: PE profiles along the O-O bond stretch and out of plane (OOP) torsional motions of the C-O-O coordinate.

Now, we return to discuss the consequences of our earlier observation of a stronger S₁ state absorption in the MACR-oxide-H₂O complex (cf. MACR-oxide). Prior studies have used CASSCF-driven surface hopping to gain insights into the excited state fate of bare MACR-oxide

following excitation to the dark S₁ state. ⁴² These latter studies reveal that cyclization to form dioxirane products is the dominant decay channel following excitation to the S₁ state. We have performed analogous surface hopping studies (but at the CASPT2 level of theory) on the MACR-oxide-H₂O complex following photoexcitation to the S₁ state. These latter simulations reveal that (as with bare MACR-oxide) the dominant decay path is cyclization (see Fig. 9). Guided by these "quick and dirty" simulations, we have calculated the PE profiles along the cyclization and O-O stretch coordinates (see Fig. 10) at the CASPT2/aug-cc-pVTZ level of theory. As evident from Fig. 10, motion along the cyclization coordinate is barrierless on the S₁ state PE surface but shows a significant barrier for O-O bond stretch. Conversely, the S₂ is bound with respect to cyclization, but reactive with respect to O-O bond stretch. Fig. 10 therefore serves as an appropriate summary for the observed trajectory results, which shows that the dominant decay process following photoexcitation to the S₁ and S₂ states is cyclization and O-O bond fission, respectively.

Table 3: Zero-point energy corrected energies of MACR-oxide unimolecular decay products relative to MACR-oxide/MACR-oxide + H₂O parent molecules, calculated at the CCSD(T)-F12/cc-pVTZ-F12//m062x/aug-cc-pVTZ level of theory. All energies are in kcal mol⁻¹.

MACR-oxide Unimolecular Decay Products	Without water complexation	With water complexation
	55.89	51.75
	55.89	51.71

-21.42	-24.53
-21.42	-24.18
-111.69	-119.96
 -106.58	-110.23
-111.69	-115.78
-106.58	-111.03
-106.58	-110.21

While the stability of the MACR-oxide-H₂O complex has been discussed previously, we now turn to compare the relative energy of various MACR-oxide unimolecular decomposition

products to their analogous H₂O complexes. The unimolecuar lifetime of the most stable MACR-oxide conformer, *anti-trans* MACR-oxide, is determined by a 1,3-ring-closing mechanism to form a dioxirane product, as both 1,4-hydrogen shift and 1,5-ring-closing reactions (in *anti* conformers) are unavailable.⁴³⁻⁴⁵ The dioxirane product may undergo further unimolecular decay, creating a bisoxy radical intermediate before forming a carboxylic acid product. As extensively discussed above, unimolecuar decay via adiabatic S₁/S₂ excitation results in O (¹D) + MACR (S₀) products via O-O bond dissociation. Table 3 displays the ground state minimum energy geometries of the aforementioned products of *anti-trans* MACR-oxide conformer alongside their relative energies both with and without H₂O complexation. The energies of the product-H₂O complexes are consistently about ~3-4 kcal mol⁻¹ lower than their bare counterparts, and they vary slightly depending upon the position of the hydrogen-bonded H₂O molecule, either approaching from the terminal hydrogen or the more allylic framework. Thus, H₂O complexation stabilizes MACR-oxide decomposition products, indicating that unimolecuar decay would occur more readily (cf. bare MACR-oxide).

Atmospheric Implications and Conclusions

We have undertaken a detailed computational study of the fate of MACR-oxide and its vdW complex with water. These present studies are motivated by laboratory studies that have shown that the lowest energy conformer of MACR-oxide is long-lived under humid conditions. The primary removal processes of atmospherically relevant CIs are unimolecular decay or bimolecular reaction with water (primarily water dimer), both of which are slow in MACR-oxide. Additionally, the extended conjugation of MACR-oxide leads to a bathochromic shift, as well as a enhanced absorption cross section, in the experimentally measured absorption profile.

This observation, along with its longer lifetime in humid conditions reinforces our hypothesis that solar photolysis may be an important sink for MACR-oxide and its vdW complex with water (MACR-oxide-H₂O).

Our results confirm that both MACR-oxide and MACR-oxide-H₂O absorb at bathochromic

wavelengths when compared to the simplest CI, formaldehyde oxide (CH₂OO). Our results also indicate that excitation to the bright S₂ state is dominated by O-O bond fission within 100 fs, although a far greater fraction of the initially excited population remains as parent MACR-oxide-H₂O complex molecules. It is likely that the remaining population undergoes O-O bond fission at a later time or may undergo unimolecular cyclization. The latter process is particularly probable if the parent molecules in the S₂ state survive for over 1 ns, which would encourage vibrational energy relaxation via collisions with inert atmospheric molecules (e.g., N₂). The nascent molecules at the minimum of S₂ may then undergo O-O bond fission or cyclization, as shown in our recent studies on adiabatically excited CH₂OO molecules. ^{19,46-49}

Interestingly, the absorption to the S₁ state in the MACR-oxide-H₂O complex is stronger than the equivalent electronic state in MACR-oxide. Given the significant overlap between the S₁ vertical excitation energy and the tropospherically relevant solar irradiance, photoexcitation to the S₁ state may be competitive at long wavelengths. The fate of the S₁ state is cyclization, which ultimately forms dioxirane products. Guided by earlier studies, the nascent dioxirane is expected to undergo subsequent unimolecular decay to form organic acids, as well as fragment products. ^{50–52}

While not mentioned previously, it is important to note that the MACR-oxide-H₂O complex is continuously being formed and destroyed, leading to an equilibrium under atmospheric conditions. If MACRO-oxide-H₂O dissociation into MACR-oxide + H₂O occurs adequately fast

enough, there could possibly be insufficient time for the complex to absorb solar photon. Thus, we aim to calculate and compare the solar photolysis lifetimes and survival rates of relevant CIcomplexes in future studies. As typical bimolecular rate constants (e.g. reaction with water) are on the order of milliseconds, we speculate that solar photolysis of these compounds, as well as their complexes with water, are on a similar or even shorter timescale. While our prior studies illustrated that CASPT2 can accurately predict the overall absorption peak position of MVKoxide and MACR-oxide, it significantly underestimates the absorption cross section by a factor of about 4. With this in mind, if we were to run a simulation of the absorption profile of MACRoxide-H₂O complex with the currently used CASPT2 method, the solar photolysis rate coefficient would be significantly underestimated, while the photolysis lifetime would be significantly overestimated. Additionally, since MACR-oxide is longer lived than typical atmospherically relevant Criegee intermediates, it may also survive to condense on secondary organic aerosol particles. Our future studies will focus on the excited state dynamics of MACRoxide at the air-water interface of atmospheric aerosol particles. This would provide better understanding of how a single water molecule versus interfacial water molecules perturbs the excited state fate of MACR-oxide.

375

376

377

378

379

380

381

359

360

361

362

363

364

365

366

367

368

369

370

371

372

373

374

Acknowledgements

The work reported in this article is supported by the National Science Foundation, under grant no. 2003422. Portions of this research were conducted with high performance computational resources provided by the Louisiana Optical Network Infrastructure (http://www.loni.org). SR thanks the Science and Engineering Research Board (SERB) under Project No. SRG/2023/001624 for the research funding.

References

- K. Sindelarova, C. Granier, I. Bouarar, A. Guenther, S. Tilmes, T. Stavrakou, J.-F. Müller, U.
 Kuhn, P. Stefani and W. Knorr, Global data set of biogenic VOC emissions calculated by the
 MEGAN model over the last 30 years, *Atmospheric Chemistry and Physics*, 2014, 14,
 9317–9341.
- T. B. Nguyen, G. S. Tyndall, J. D. Crounse, A. P. Teng, K. H. Bates, R. H. Schwantes, M. M.
 Coggon, L. Zhang, P. Feiner, D. O. Milller, K. M. Skog, J. C. Rivera-Rios, M. Dorris, K. F.
 Olson, A. Koss, R. J. Wild, S. S. Brown, A. H. Goldstein, J. A. De Gouw, W. H. Brune, F. N.
 Keutsch, J. H. Seinfeld and P. O. Wennberg, Atmospheric fates of Criegee intermediates in
 the ozonolysis of isoprene, *Physical Chemistry Chemical Physics*, 2016, 18, 10241–10254.
- 393 S. M. Aschmann and Roger. Atkinson, Formation Yields of Methyl Vinyl Ketone and
 394 Methacrolein from the Gas-Phase Reaction of O3 with Isoprene, *Environmental Science & Technology*, 1994, **28**, 1539–1542.
- R. Gutbrod, E. Kraka, R. N. Schindler and D. Cremer, Kinetic and Theoretical Investigation of the Gas-Phase Ozonolysis of Isoprene: Carbonyl Oxides as an Important Source for OH Radicals in the Atmosphere, *Journal of the American Chemical Society*, 1997, **119**, 7330–399
- H. K. Lee, P. Chantanapongvanij, R. R. Schmidt and T. A. Stephenson, Master Equation
 Studies of the Unimolecular Decay of Thermalized Methacrolein Oxide: The Impact of
 Atmospheric Conditions, *The Journal of Physical Chemistry A*, 2023, 127, 4492–4502.
- K. T. Kuwata and L. C. Valin, Quantum chemical and RRKM/master equation studies of isoprene ozonolysis: Methacrolein and methacrolein oxide, *Chemical Physics Letters*, 2008, **451**, 186–191.
- V. P. Barber, S. Pandit, A. M. Green, N. Trongsiriwat, P. J. Walsh, S. J. Klippenstein and M. I.
 Lester, Four-Carbon Criegee Intermediate from Isoprene Ozonolysis: Methyl Vinyl Ketone
 Oxide Synthesis, Infrared Spectrum, and OH Production, *Journal of the American* Chemical Society, 2018, 140, 10866–10880.
- M. F. Vansco, R. L. Caravan, K. Zuraski, F. A. F. Winiberg, K. Au, N. Trongsiriwat, P. J. Walsh,
 D. L. Osborn, C. J. Percival, M. A. H. Khan, D. E. Shallcross, C. A. Taatjes and M. I. Lester,
 Experimental Evidence of Dioxole Unimolecular Decay Pathway for Isoprene-Derived
 Criegee Intermediates, *Journal of Physical Chemistry A*, 2020, 124, 3542–3554.
- R. L. Caravan, M. F. Vansco, K. Au, M. A. H. Khan, Y.-L. Li, F. A. F. Winiberg, K. Zuraski, Y.-H.
 Lin, W. Chao, N. Trongsiriwat, P. J. Walsh, D. L. Osborn, C. J. Percival, J. J.-M. Lin, D. E.
 Shallcross, L. Sheps, S. J. Klippenstein, C. A. Taatjes and M. I. Lester, Direct kinetic
 measurements and theoretical predictions of an isoprene-derived Criegee intermediate, *Proceedings of the National Academy of Sciences*, 2020, 117, 9733 LP 9740.
- Y.-H. Lin, C. Yin, K. Takahashi and J. J.-M. Lin, Surprisingly long lifetime of methacrolein
 oxide, an isoprene derived Criegee intermediate, under humid conditions,
 Communications Chemistry, 2021, 4, 12.

- 422 11 R. L. Caravan, M. F. Vansco and M. I. Lester, Open questions on the reactivity of Criegee intermediates, *Communications Chemistry*, 2021, **4**, 44.
- 424 12 M. F. Vansco, B. Marchetti and M. I. Lester, Electronic spectroscopy of methyl vinyl ketone 425 oxide: A four-carbon unsaturated Criegee intermediate from isoprene ozonolysis, *Journal* 426 *of Chemical Physics*, 2018, **149**, 244309.
- M. F. Vansco, B. Marchetti, N. Trongsiriwat, T. Bhagde, G. Wang, P. J. Walsh, S. J.
 Klippenstein and M. I. Lester, Synthesis, Electronic Spectroscopy, and Photochemistry of
 Methacrolein Oxide: A Four-Carbon Unsaturated Criegee Intermediate from Isoprene
 Ozonolysis, Journal of the American Chemical Society, 2019, 141, 15058–15069.
- 431 14 W. L. Ting, Y. H. Chen, W. Chao, M. C. Smith and J. J. M. Lin, The UV absorption spectrum 432 of the simplest Criegee intermediate CH 200, *Physical Chemistry Chemical Physics*, 2014, 433 **16**, 10438–10443.
- 434 15 Y. H. Lin, K. Takahashi and J. J. M. Lin, Absolute photodissociation cross sections of 435 thermalized methyl vinyl ketone oxide and methacrolein oxide, *Physical Chemistry* 436 *Chemical Physics*, 2022, **24**, 10439–10450.
- J. C. McCoy, S. J. Leger, C. F. Frey, M. D. Vansco, B. Marchetti and T. N. V. Karsili, Modeling the Conformer-Dependent Electronic Absorption Spectra and Photolysis Rates of Methyl Vinyl Ketone Oxide and Methacrolein Oxide, *Journal of Physical Chemistry A*, 2022, **126**, 485–496.
- 441 17 K. Takahashi, Wave Packet Calculation of Absolute UV Cross Section of Criegee 442 Intermediates, *The Journal of Physical Chemistry A*, 2022, **126**, 6080–6090.
- 443 18 G. Wang, T. Liu, A. Caracciolo, M. F. Vansco, N. Trongsiriwat, P. J. Walsh, B. Marchetti, T. N. V Karsili and M. I. Lester, Photodissociation dynamics of methyl vinyl ketone oxide: A four-carbon unsaturated Criegee intermediate from isoprene ozonolysis., *The Journal of chemical physics*, 2021, **155**, 174305.
- V. J. Esposito, L. Tianlin, G. Wang, A. Caracciolo, M. F. Vansco, B. Marchetti, T. N. V. Karsili
 and M. I. Lester, Photodissociation Dynamics of CH2OO on Multiple Potential Energy
 Surfaces: Experiment and Theory, *The Journal of Physical Chemistry A*, ,
 DOI:10.1021/acs.jpca.1c03643.
- 451 20 M. J. Frisch, G. W. Trucks, H. B. Schlegel, G. E. Scuseria, M. A. Robb, J. R. Cheeseman, G.
- Scalmani, V. Barone, B. Mennucci, G. A. Petersson, H. Nakatsuji, M. Caricato, X. Li, H. P.
- 453 Hratchian, A. F. Izmaylov, J. Bloino, G. Zheng, J. L. Sonnenberg, M. Hada, M. Ehara, K.
- Toyota, R. Fukuda, J. Hasegawa, M. Ishida, T. Nakajima, Y. Honda, O. Kitao, H. Nakai, T.
- Vreven, J. A. Montgomery Jr., J. E. Peralta, F. Ogliaro, M. Bearpark, J. J. Heyd, E. Brothers, K. N. Kudin, V. N. Staroverov, R. Kobayashi, J. Normand, K. Raghavachari, A. Rendell, J. C.
- 456 K. N. Kudin, V. N. Staroverov, R. Kobayashi, J. Normand, K. Raghavachari, A. Rendell, J. C. Burant, S. S. Iyengar, J. Tomasi, M. Cossi, N. Rega, N. J. Millam, M. Klene, J. E. Knox, J. B.
- 458 Cross, V. Bakken, C. Adamo, J. Jaramillo, R. Gomperts, R. E. Stratmann, O. Yazyev, A. J.
- 459 Austin, R. Cammi, C. Pomelli, J. W. Ochterski, R. L. Martin, K. Morokuma, V. G. Zakrzewski,
- 460 G. A. Voth, P. Salvador, J. J. Dannenberg, S. Dapprich, A. D. Daniels, Ö. Farkas, J. B.
- Foresman, J. V Ortiz, J. Cioslowski and D. J. Fox, Gaussian 16, Revision C.01, *Gaussian Inc. Wallingford CT*.
- 463 21 M. J. Frisch, G. W. Trucks, H. B. Schlegel, G. E. Scuseria, M. A. Robb, J. R. Cheeseman, G.
- Scalmani, V. Barone, B. Mennucci, G. A. Petersson, H. Nakatsuji, M. Caricato, X. Li, H. P.
- 465 Hratchian, A. F. Izmaylov, J. Bloino, G. Zheng, J. L. Sonnenberg, M. Hada, M. Ehara, K.

- Toyota, R. Fukuda, J. Hasegawa, M. Ishida, T. Nakajima, Y. Honda, O. Kitao, H. Nakai, T.
- Vreven, J. A. Montgomery Jr., J. E. Peralta, F. Ogliaro, M. Bearpark, J. J. Heyd, E. Brothers,
- 468 K. N. Kudin, V. N. Staroverov, R. Kobayashi, J. Normand, K. Raghavachari, A. Rendell, J. C.
- Burant, S. S. Iyengar, J. Tomasi, M. Cossi, N. Rega, N. J. Millam, M. Klene, J. E. Knox, J. B.
- 470 Cross, V. Bakken, C. Adamo, J. Jaramillo, R. Gomperts, R. E. Stratmann, O. Yazyev, A. J.
- 471 Austin, R. Cammi, C. Pomelli, J. W. Ochterski, R. L. Martin, K. Morokuma, V. G. Zakrzewski,
- 472 G. A. Voth, P. Salvador, J. J. Dannenberg, S. Dapprich, A. D. Daniels, Ö. Farkas, J. B.
- 473 Foresman, J. V Ortiz, J. Cioslowski and D. J. Fox, 2016, Gaussian 16, Revision A.03,
- 474 Gaussian, Inc.
- 475 22 Y. Zhao and D. G. Truhlar, The M06 suite of density functionals for main group
- 476 thermochemistry, thermochemical kinetics, noncovalent interactions, excited states, and
- 477 transition elements: two new functionals and systematic testing of four M06-class
- functionals and 12 other functionals, *Theoretical Chemistry Accounts*, 2008, **120**, 215–
- 479 241.
- 480 23 L. Vereecken, A. R. Rickard, M. J. Newland and W. J. Bloss, Theoretical study of the
- reactions of Criegee intermediates with ozone, alkylhydroperoxides, and carbon
- 482 monoxide, *Physical Chemistry Chemical Physics*, 2015, **17**, 23847–23858.
- 483 24 L. Vereecken, H. Harder and A. Novelli, The reactions of Criegee intermediates with
- alkenes, ozone, and carbonyl oxides, *Physical Chemistry Chemical Physics*, 2014, **16**, 4039–4049.
- 486 25 H.-J. Werner, P. J. Knowles, G. Knizia, F. R. Manby and M. Schütz, Molpro: a general-
- purpose quantum chemistry program package, *WIREs Computational Molecular Science*, 2012, **2**, 242–253.
- 489 26 B. O. Roos, P. Linse, P. E. M. Siegbahn and M. R. A. Blomberg, A simple method for the
- evaluation of the second-order-perturbation energy from external double-excitations with a CASSCF reference wavefunction, *Chemical Physics*, 1982, **66**, 197–207.
- 492 27 Kerstin. Andersson, P. Aake. Malmqvist, B. O. Roos, A. J. Sadlej and Krzysztof. Wolinski,
- Second-order perturbation theory with a CASSCF reference function, *The Journal of*
- 494 *Physical Chemistry*, 1990, **94**, 5483–5488.
- 495 28 K. Andersson, P. Malmqvist and B. O. Roos, Second-order perturbation theory with a
- complete active space self-consistent field reference function, *The Journal of Chemical*
- 497 *Physics*, 1992, **96**, 1218–1226.
- 498 29 T. H. Dunning, Gaussian basis sets for use in correlated molecular calculations. I. The
- atoms boron through neon and hydrogen, *The Journal of Chemical Physics*, 1989, **90**,
- 500 1007–1023.
- 501 30 B. O. Roos, P. R. Taylor and P. E. M. Sigbahn, A complete active space SCF method
- 502 (CASSCF) using a density matrix formulated super-CI approach, *Chemical Physics*, 1980,
- **48**, 157–173.
- B. O. Roos, The complete active space SCF method in a fock-matrix-based super-Cl formulation, *International Journal of Quantum Chemistry*, 1980, **18**, 175–189.
- 506 32 J. C. Tully, Molecular dynamics with electronic transitions, *The Journal of Chemical*
- 507 *Physics*, 1990, **93**, 1061–1071.

- M. Barbatti, M. Ruckenbauer, F. Plasser, J. Pittner, G. Granucci, M. Persico and H. Lischka,
 Newton-X: A surface-hopping program for nonadiabatic molecular dynamics, *Wiley Interdisciplinary Reviews: Computational Molecular Science*, 2014, 4, 26–33.
- 511 34 E. Antwi, R. E. Bush, B. Marchetti and T. N. V Karsili, A direct dynamics study of the exotic photochemistry of the simplest Criegee intermediate, CH2OO, *Phys. Chem. Chem. Phys.*, 2022, **24**, 16724–16731.
- J. Woo Park and T. Shiozaki, Analytical Derivative Coupling for Multistate CASPT2 Theory, *J Chem Theory Comput*, 2017, **13**, 2561–2570.
- 516 36 L. Sheps, B. Rotavera, A. J. Eskola, D. L. Osborn, C. A. Taatjes, K. Au, D. E. Shallcross, M. A. H. Khan and C. J. Percival, The reaction of Criegee intermediate CH2OO with water dimer: Primary products and atmospheric impact, *Physical Chemistry Chemical Physics*, 2017, **19**, 21970–21979.
- R. Yajima, Y. Sakamoto, S. Inomata and J. Hirokawa, Relative Reactivity Measurements of Stabilized CH2OO, Produced by Ethene Ozonolysis, Toward Acetic Acid and Water Vapor Using Chemical Ionization Mass Spectrometry, *The Journal of Physical Chemistry A*, 2017, 121, 6440–6449.
- T. R. Lewis, M. A. Blitz, D. E. Heard and P. W. Seakins, Direct evidence for a substantive reaction between the Criegee intermediate, CH2OO, and the water vapour dimer,
 Physical Chemistry Chemical Physics, 2015, 17, 4859–4863.
- 527 39 T. Berndt, J. Voigtländer, F. Stratmann, H. Junninen, R. L. Mauldin III, M. Sipilä, M. Kulmala 528 and H. Herrmann, Competing atmospheric reactions of CH2OO with SO2 and water 529 vapour, *Phys. Chem. Chem. Phys.*, 2014, **16**, 19130–19136.
- 530 40 W. Chao, J.-T. Hsieh, C.-H. Chang and J. J.-M. Lin, Atmospheric chemistry. Direct kinetic 531 measurement of the reaction of the simplest Criegee intermediate with water vapor., 532 *Science (New York, N.Y.)*, 2015, **347**, 751–754.
- 533 41 M. C. Smith, C.-H. Chang, W. Chao, L.-C. Lin, K. Takahashi, K. A. Boering and J. J.-M. Lin, 534 Strong Negative Temperature Dependence of the Simplest Criegee Intermediate 535 CH2OO Reaction with Water Dimer., *The journal of physical chemistry letters*, 2015, **6**, 536 2708–2713.
- J. Yang, Y. Li, L. Makroni and F. Liu, The photoisomerization mechanism of methacrolein oxide (MACR-OO): the cyclic dioxole formation pathway revealed, *Physical Chemistry Chemical Physics*, 2022, **24**, 22531–22537.
- 540 43 K. T. Kuwata and L. C. Valin, Quantum chemical and RRKM/master equation studies of 541 isoprene ozonolysis: Methacrolein and methacrolein oxide, *Chem Phys Lett*, 2008, **451**, 542 186–191.
- M. F. Vansco, B. Marchetti, N. Trongsiriwat, T. Bhagde, G. Wang, P. J. Walsh, S. J.
 Klippenstein and M. I. Lester, Synthesis, Electronic Spectroscopy, and Photochemistry of
 Methacrolein Oxide: A Four-Carbon Unsaturated Criegee Intermediate from Isoprene
 Ozonolysis, J Am Chem Soc, 2019, 141, 15058–15069.
- 547 45 L. Vereecken, A. Novelli and D. Taraborrelli, Unimolecular decay strongly limits the 548 atmospheric impact of Criegee intermediates, *Physical Chemistry Chemical Physics*, 2017, 549 **19**, 31599–31612.

- J. H. Lehman, H. Li, J. M. Beames and M. I. Lester, Communication: Ultraviolet
 photodissociation dynamics of the simplest Criegee intermediate CH2OO, *The Journal of Chemical Physics*, 2013, 139, 141103.
- 553 47 E. Antwi, R. Bush, B. Marchetti and T. Karsili, A direct dynamics study of the exotic 554 photochemistry of the simplest Criegee intermediate, CH2OO, *Physical Chemistry* 555 *Chemical Physics*, 2022, **24**, 16724–16731.
- 556 48 V. J. Esposito, O. Werba, S. A. Bush, B. Marchetti and T. N. V Karsili, Insights into the Ultrafast Dynamics of CH2OO and CH3CHOO Following Excitation to the Bright $1\pi\pi^*$ State: The Role of Singlet and Triplet States, *Photochemistry and Photobiology*, , DOI:https://doi.org/10.1111/php.13560.
- E. Antwi, J. M. Ratliff, M. N. R. Ashfold and T. N. V. Karsili, Comparing the Excited State
 Dynamics of CH2OO, the Simplest Criegee Intermediate, Following Vertical versus
 Adiabatic Excitation, *The journal of physical chemistry. A*, 2022, **126**, 6236–6243.
- 563 D. L. Osborn and C. A. Taatjes, The physical chemistry of Criegee intermediates in the gas 564 phase, *International Reviews in Physical Chemistry*, 2015, **34**, 309–360.
- K. T. Kuwata, M. R. Hermes, M. J. Carlson and C. K. Zogg, Computational Studies of the
 Isomerization and Hydration Reactions of Acetaldehyde Oxide and Methyl Vinyl Carbonyl
 Oxide, *The Journal of Physical Chemistry A*, 2010, **114**, 9192–9204.
- J. M. Anglada, J. M. Bofill, S. Olivella and A. Solé, Unimolecular Isomerizations and Oxygen
 Atom Loss in Formaldehyde and Acetaldehyde Carbonyl Oxides. A Theoretical
 Investigation, Journal of the American Chemical Society, 1996, 118, 4636–4647.